Diagnostic Utility of Diffusion-weighted Magnetic Resonance Imaging in Differentiating Small Solid Renal Tumors (≤4 cm) at 3.0T Magnetic Resonance Imaging

Han-Mei Zhang[1], Ying-Hua Wu[2], Qi Gan[3], Xiao Lyu[4], Xiang-Lan Zhu[5], Min Kuang[2], Rong-Bo Liu[1], Zi-Xing Huang[1], Fang Yuan[1], Xi-Jiao Liu[1], Bin Song[1]

[1]Department of Radiology, West China Hospital, Sichuan University, Chengdu, Sichuan 610041, China
[2]Department of Radiology, The Second Clinical Medicine School, Chengdu University of Traditional Chinese Medicine, Chengdu, Sichuan 610041, China
[3]Department of Neurosurgery, West China Hospital, Sichuan University, Chengdu, Sichuan 610041, China
[4]Department of Urology, West China Hospital, Sichuan University, Chengdu, Sichuan 610041, China
[5]Department of Pathology, West China Hospital, Sichuan University, Chengdu, Sichuan 610041, China

Han-Mei Zhang and Ying-Hua Wu contributed equally.

Abstract

Background: The aim of this study was to assess the performance of apparent diffusion coefficient (ADC) measurement obtained with diffusion-weighted magnetic resonance imaging (DW-MRI) to distinguish renal cell carcinomas (RCCs) from small benign solid renal tumors (≤4 cm).

Methods: In this cross-sectional study, 49 consecutive patients with histopathologically confirmed small solid renal tumors, and seven healthy volunteers were imaged using nonenhanced MRI and DW-MRI. The ADC map was calculated using the b values of 0, 50, 400, and 600 s/mm^2 and values compared via the Kruskal–Wallis and Mann–Whitney tests. The utility of ADC for differentiating RCCs and benign lesions was assessed using a receiver operating characteristic curve. Multiple nonenhanced MRI features were analyzed by Logistic regression.

Results: The tumors consisted of 33 cases of clear-cell RCCs (ccRCCs) and 16 cases of benign tumors, including 14 cases of minimal fat angiomyolipomas and 2 cases of oncocytomas. The ADCs showed significant differences among benign tumors ([0.90 ± 0.52] × 10^{-3} mm^2/s), ccRCCs ([1.53 ± 0.31] × 10^{-3} mm^2/s) and the normal renal parenchyma ([2.22 ± 0.12] × 10^{-3} mm^2/s) ($P < 0.001$). Moreover, there was statistically significant difference between high and low-grade ccRCCs ($P = 0.004$). Using a cut-off ADC of 1.36×10^{-3} mm^2/s, DW-MRI resulted in an area under the curve (AUC), sensitivity, and specificity equal to 0.839, 75.8%, and 87.5%, respectively. Nonenhanced MRI alone and the combination of imaging methods led to an AUC, sensitivity and specificity equal to 0.919, 93.9%, and 81.2%, 0.998, 97%, and 100%, respectively. The Logistic regression showed that the location of the center of the tumor (inside the contour of the kidney) and appearance of stiff blood vessel were significantly helpful for diagnosing ccRCCs.

Conclusions: DW-MRI has potential in distinguishing ccRCCs from benign lesions in human small solid renal tumors (≤4 cm), and in increasing the accuracy for diagnosing ccRCCs when combined with nonenhanced MRI.

Key words: Apparent Diffusion Coefficient Value; Diffusion-weighted Magnetic Resonance Imaging; Renal Cell Carcinomas; Renal Tumors

INTRODUCTION

It is necessary to accurately diagnose renal cell carcinoma (RCC) for early intervention and improved prognosis.[1] Currently, contrast-enhancement computed tomography (CE-CT) and CE magnetic resonance imaging (CE-MRI) are the two main imaging techniques used to evaluate RCC characteristics,[2] but the risk of contrast material–induced nephropathy by CE-CT[3] and

nephrogenic systemic fibrosis with renal insufficiency by CE-MRI[4] have been of increasing concern. Thus, there is a need for noninvasive and nonenhanced imaging techniques to diagnose and distinguish the features of renal tumors.

Diffusion-weighted MRI (DW-MRI) has been widely applied to distinguish benign and malignant tumors. This technique derives from the restriction of the random Brownian motion of water molecules in tissue by interactions with cell membranes and macromolecules. The apparent diffusion coefficient (ADC) is a measurement of the magnitude of diffusion of the tissue water, which can be used to quantitative

Address for correspondence: Dr. Bin Song,
Department of Radiology, West China Hospital, Sichuan University,
Chengdu, Sichuan 610041, China
E-Mail: cjr.songbin@vip.163.com

pathological changes without contrast. Some studies have shown that the ADC obtained from DW imaging (DWI) can help differentiate various renal masses, and has a certain value in classification and grading of RCC.[5-9] However, few studies have focused on the capability of DW-MRI for the early and differential diagnosis of renal tumors 4 cm or smaller in size, the criterion widely used in clinical practice for the tumor node metastasis (TNM) staging of RCC.[10] In addition, few investigators have assessed the accuracy of DW-MRI combined with nonenhanced MRI for RCC characterization.

According to the TNM 7th edition, UICC/AJCC TNM staging system, T1a renal tumors are ≤4 cm.[11] Accurately identifying tumors at that stage results in an early intervention an improved prognosis. We hypothesized that DW-MRI could yield more comprehensive information than nonenhanced MRI in characterizing human small solid renal tumors (≤4 cm). Thus, the purpose of this study was to assess the performance of ADC measurements obtained with DW-MRI to characterize human small solid renal tumors (≤4 cm) that have a histopathology diagnosis.

METHODS

Patients

This was a cross-sectional study performed from March 2011 to April 2014 in the West China Hospital of Sichuan University. The hospital ethics committee approved the study protocol. All cases met the inclusion criteria: (i) Ultrasound or abdominal CT scanning indicated single solid renal lesion, and the diameter of each lesion did not exceed 4 cm; (ii) the patients had not undergone biopsy or any treatment for renal lesion prior to MRI; and (iii) the age of all cases varied from 18 to 70 years.[12] The exclusion criteria of patients were as follows: (i) Patients who had contraindication for MRI examination; (ii) patients who had cardiac or renal insufficiency; and (iii) patients who did not undergo operation or postsurgical histopathology or renal lesions were not tumors confirmed by histopathology. The case group consisted of 49 consecutive patients, including 26 males and 23 females, ranging in age from 21 to 70 years. The patients, who had solid renal tumors found on ultrasound, underwent MRI for further evaluation [Figure 1]. Tumor type was confirmed by postsurgical histopathology. The control group consisted of seven healthy volunteers, ranging in age from 18 to 70 years.

Magnetic resonance imaging protocol

Magnetic resonance imaging was performed using a Siemens 3.0T MR scanner with torso phased-array coils including nonenhanced MRI and breath-hold DWI on all patients and healthy volunteers. All subjects underwent coronal HASTE T2-weighted image (T2WI), axial TSE T2WI and axial GRE T1WI (in-phase and out-of-phase). The parameters were as follows: Coronal T2WI: Repetition time (TR) 1000 ms, echo time (TE) 90 ms, matrix 320 × 256; NEX 1; field of view (FOV) 452 × 452 mm; slice thickness 3 mm; axial T2WI: TR 1800 ms, TE 95 ms, matrix 320 × 256; NEX 1; FOV 378 × 276 mm; slice thickness 5 mm; axial T1WI: TR 150 ms, TE 2.2/3.6 ms, matrix 256 × 205; NEX 1; FOV 438 × 285 mm; slice thickness 5 mm.
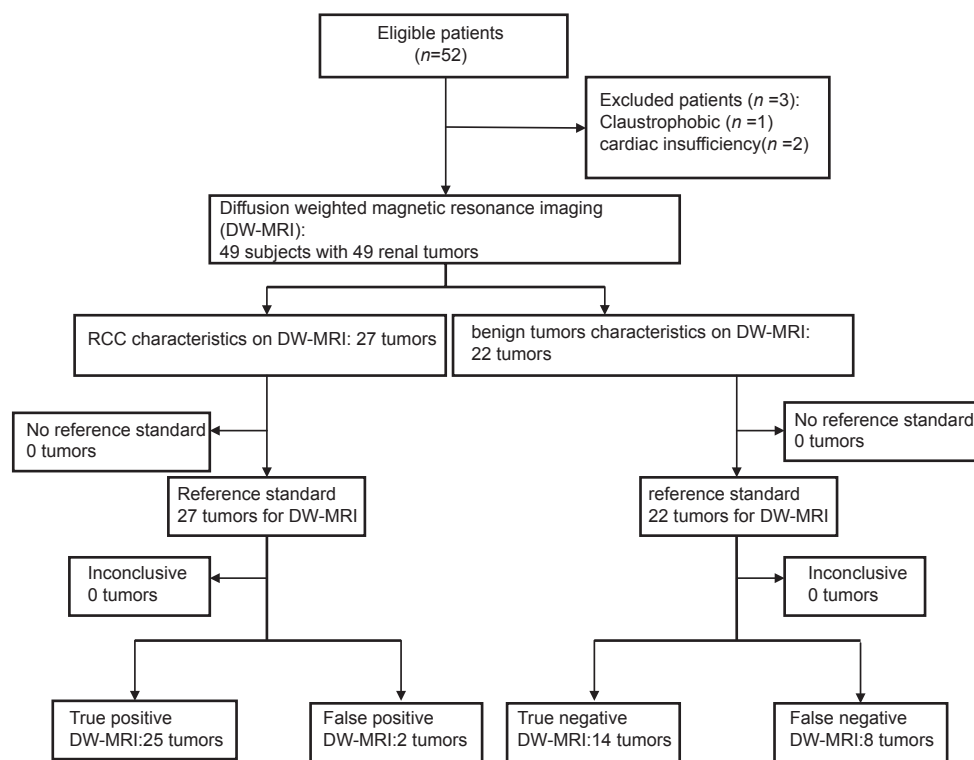

Figure 1: Flowchart outlines patient population, diffusion-weighted-magnetic resonance imaging for diagnosing renal cell carcinoma, and reference-standard findings.

For DW-MRI, breath-hold image acquisitions were performed in the transverse plane using a fat-suppressed echo-planar imaging sequence with tri-directional gradients and multiple b values: 0, 50, 400 and 600 s/mm². The parameters were as follows: TR = 800 ms, TE = 73 ms, matrix = 192 × 154; NEX = 2; FOV = 393 × 295 mm; slice thickness 3 mm; total acquisition time 60 s. The MRI parameters are listed in Table 1.

Imaging study
Magnetic resonance imaging
Two experienced abdominal radiologists reviewed the images in consensus at a commercially available workstation (Syngo). All renal tumors were characterized on the basis of signal intensity on T1WI and T2WI.[13] The main features of nonenhanced MRI were observed, including location of lesions, signal intensity of lesions, necrosis of tumors, the lifted cortex, the angular interface and stiff vessels within tumors, etc.[14] Ultimately, renal tumors were judged to be presumably RCC or presumably benign.

Diffusion-weighted-magnetic resonance imaging
Another experienced radiologist, blinded, evaluated the ADC values of renal tumors in the Syngo workstation. The mean ADC values of the renal tumors were measured using regions of interest, which were placed over the largest region possible of the renal tumors as large as possible while avoiding regions of necrosis and cystic degeneration.[15] Three measurements were performed per tumor while the ADC values of normal renal cortex were measured in three locations (upper, middle, and lower pole) in each kidney.

Reference standard
All tumors were confirmed by post operational histopathology. Diagnosis standard of RCC is the Fuhrman classification system with a nuclear grade of the tumor by an experienced pathologist. A two-tiered classification system was established: low-grade, which included grades I and II, and high-grade, which included grades III and IV.[16]

Statistical analyses
Statistical analyses were performed using SPSS software (version 22, SPSS, IBM, USA). The Kruskal–Wallis test and Mann–Whitney test were used to determine the significance of differences in ADCs between renal tumors and normal renal parenchyma, and to compare the significance of differences in ADCs of high-grade RCCs and low-grade RCCs. The receiver operating characteristic (ROC) analysis was used to assess the utility of ADC for detecting RCCs from benign tumors. The threshold value for ADC measurement that yielded the highest average sensitivity and specificity was identified for all tumors. Moreover, a Logistic regression model was used to find the most valuable features among the nonenhanced MRI features. All reported P values were two-sided and considered to be statistically significant when <0.05.

RESULTS
General characteristics
Each patient had a solitary renal tumor, and the average diameter of the 49 renal tumors was 3.2 ± 1.16 cm. The tumors consisted of 33 cases of clear-cell RCCs (ccRCCs) and 16 cases of benign tumors, which included 14 cases of minimal fat angiomyolipomas (MFAMLs) and 2 cases of oncocytomas. All tumor classifications were confirmed by postsurgical histopathology [Figure 2]. No significant difference was found in the age or sex of patients with these tumors ($P > 0.05$).

Apparent diffusion coefficient value
We compared diffusion in normal renal parenchyma and small solid renal tumors. DWI was performed using b values of 0, 50, 400, 600 s/mm², and the ADC values determined based on three measurements per tumor or three locations per normal kidney cortex [Figure 3]. Using a pair-wise comparison, we found that both the ccRCCs and benign tumors displayed restricted diffusion as compared with the normal parenchyma and that these differences were statistically significant [Table 2]. Moreover, the mean ADC value of the ccRCCs ($[1.53 \pm 0.31] \times 10^{-3}$ mm²/s) was higher than that of benign tumors ($[0.90 \pm 0.52] \times 10^{-3}$ mm²/s) ($P = 0.001$). Separating the ccRCCs into high and low Furman grades revealed that the mean ADC value of the low-grade ccRCCs ($[1.65 \pm 0.26] \times 10^{-3}$ mm²/s) was significantly higher than that of the high-grade ccRCCs ($[1.32 \pm 0.29] \times 10^{-3}$ mm²/s) ($P = 0.004$).

Table 1: Imaging parameters for DW-MRI and nonenhanced MRI sequences

Parameter	DW imaging	Coronal T2WI	Axial T2WI	Axial T1WI
Repetition time (ms)	800	1000	1800	150
Echo time (ms)	73	90	95	2.2/3.6
Flip angle (degrees)	–	150	140	65
Section thickness (mm)	3	3	5	5
Matrix	192 × 154	320 × 256	320 × 256	256 × 205
Field of view (mm)	393 × 295	452 × 452	378 × 276	438 × 285
Number of signals acquired	2	1	1	1
Echo-planar imaging factor	115	–	–	–
Acquisition time (s)	60, three sessions of 20 s each	15	36	23

DW-MRI: Diffusion-weighted magnetic resonance imaging; T1WI: T1-weighted image; T2WI: T2-weighted image.
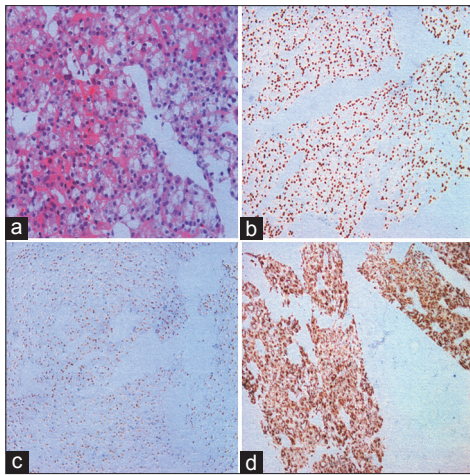
Figure 2: (a) H and E staining in clear-cell renal cell carcinoma (ccRCC). Panels refer to representative sections showing cubic, wedge-shaped, and large volume of tumor cells; circular, oval, and centered cell nucleus, exquisite chromatin, visible nucleoli, lucid cytoplasm (original magnification × 400); (b and c) Immunohistochemical staining of PAX8 and PAX2 in ccRCC. Panels refer to representative sections showing positive cell nucleus staining; (d) Immunohistochemical staining of RCC in ccRCC. Panels refer to representative sections showing positive cell membrane strong staining.

Receiver operating characteristic curve

We generated a ROC curve to compare the performance of DW-MRI alone, nonenhanced MRI alone and a combination of the two imaging methods for diagnosing ccRCC [Figure 4]. Using a cut-off ADC of 1.36×10^{-3} mm²/s, DW-MRI resulted in an area under the curve (AUC), sensitivity, and specificity equal to 0.839, 75.8%, and 87.5%, respectively. Nonenhanced MRI led to an AUC, sensitivity, and specificity equal to 0.919, 93.9%, and 81.2%, respectively. Finally, the combination of imaging methods produced an AUC, sensitivity, and specificity equal to 0.998, 97%, and 100%, respectively.

Features of nonenhanced magnetic resonance imaging

The Logistic regression showed that the location of center of the tumor (inside the contour of the kidney) ($P < 0.001$) and appearance of stiff blood vessels ($P = 0.01$) were significantly helpful for diagnosing ccRCCs. We found that the signal intensity of lesions, necrosis of tumors, the lifted cortex, and the angular interface had no significant effect on diagnosing ccRCCs in our study.

DISCUSSION

This study supports the potential utility of DW-MRI for the characterization of ccRCCs in human small solid renal tumors (≤4 cm). Currently, CE-CT and CE-MRI are the two conventional imaging techniques used to evaluate RCC characteristics,[2] while dynamic CE-CT and MRI are serving as the "gold standard" for solid renal mass differentiation.[17,18] Mileto et al.[19] reported that CE dual-energy MDCT with iodine-related attenuation and iodine quantification allows accurate evaluation of iodine uptake in renal lesions on a single-phase nephrographic image, which could reach a
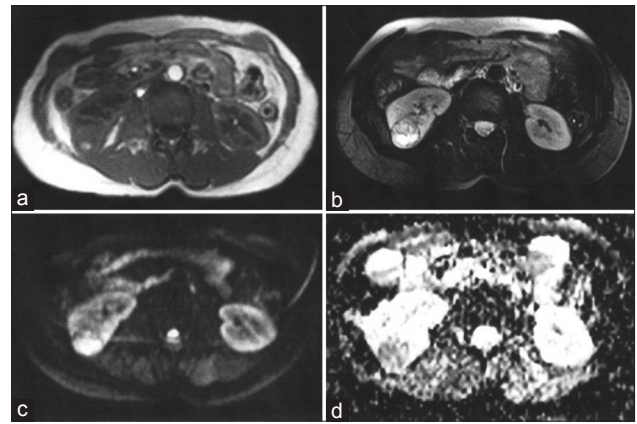

Figure 3: Clear-cell renal cell carcinoma image (ccRCC) of nonenhanced conventional magnetic resonance imaging (MRI) and diffusion-weighted-MRI (DW-MRI) in a 54-year-old woman. (a) T1-weighted image; (b) T2-weighted image; (c) Transverse fat-suppressed echo-planar DW images show right renal mass that is relatively hyperintense; (d) On transverse apparent diffusion coefficient (ADC) map, mean ADC for *b* values of 0, 50, 400, and 600 s/mm² is visually lower in renal mass than in renal cortex.

sensitivity and specificity of 100% and 97.7%, respectively. Kim et al.[20] included 466 nonfatty solid renal masses to evaluate the clinico-radio-pathologic features of a solitary solid renal mass at MDCT examination and concluded that MDCT accuracy for detection of RCC was 94%. In our study, the AUC, sensitivity, and specificity of nonenhanced MRI for diagnosing ccRCCs were 0.919, 93.9%, and 81.2%, respectively, while the AUC, sensitivity, and specificity of DW-MRI combined with nonenhanced MRI for diagnosing ccRCCs were 0.998, 97%, and 100%, respectively. This indicated that DW-MRI provided additional information to that acquired with nonenhanced MRI, and the combination yielded a diagnostic accuracy similar to that of CE-CT. In addition, use of DW-MRI and nonenhanced MRI could also decrease the risk of contrast-induced nephropathy and nephrogenic systemic fibrosis in CE-CT or CE-MRI,[21,22] supporting its potential.

The ADCs both in ccRCCs and benign renal tumors were lower than in normal renal parenchyma. This finding indicates that the motion of water molecules in tumors was more restricted than in normal renal parenchyma. This may be explained by the observation that tissue with high cellular density and numerous intact cell membranes have a greater restriction of the water molecule motion.[15] MFAMLs comprised 87.5% of the benign tumors in our study. Our observation that the benign tumors had a lower mean ADC than the ccRCCs could be explained by the fact that muscle and other solid components restrict diffusion.[23] Moreover, we found differences in ADC values when we subdivided the ccRCCs into high and low grades based on the Fuhrman grading system that uses nuclear features. The Fuhrman grading system for ccRCC is based exclusively on nuclear features, specifically nuclear irregularity, nuclear size, and nucleolar prominence; high grades often show large complex-shaped nuclei with prominent nucleoli

Table 2: Comparisons of ADCs values

Category	ADC (×10⁻³ mm²/s)*	P
Benign tumors versus ccRCCs†	0.90 ± 0.52 versus 1.53 ± 0.31	0.001
ccRCCs versus normal renal parenchyma	1.53 ± 0.31 versus 2.22 ± 0.12	0.001
Benign tumors versus normal renal parenchyma	0.90 ± 0.52 versus 2.22 ± 0.12	<0.001
Low Furman grade versus high Furman grade of ccRCCs	1.65 ± 0.26 vesus 1.32 ± 0.29	0.004

*Data are means ± SD; †ccRCC: Clear cell renal cell carcinoma; SD: Standard deviation; ADC: Apparent diffusion coefficient.
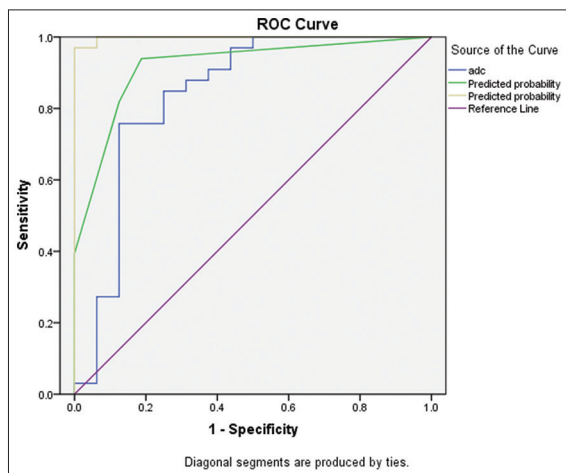

Figure 4: Receiver operating characteristic curves for diffusion-weighted-magnetic resonance imaging (MRI), nonenhanced MRI alone and a combination of the two imaging methods.

and possibly heavy chromatin clumps.[16] Meanwhile, the generalized estimating equation analysis based on a Logistic regression model indicated that the center location of tumors inside the contour of the kidney and the appearance of stiff blood vessels were remarkably helpful for the diagnosis of ccRCCs.

Previous studies reported the diagnostic utility of DW-MRI in the identification of the renal diseases like hydronephrosis and pyonephrosis,[24] and determination of renal tumors when DW-MRI was combined with CE-MRI.[13] Taouli et al.[13] reported that the AUC, sensitivity, and specificity of DW-MRI for diagnosing RCCs (excluding angiomyolipomas) were 0.856, 86%, and 80%, respectively. The AUC and sensitivity were higher than our results, which may be due to our small sample size and the different categories of benign lesions in our study. In addition, Taouli's study demonstrated the mean ADC of RCCs was significantly lower than that of benign lesions ($P < 0.0001$), which contradicts our result. There are several potential reasons for this difference: (i) In Taouli's study, 80% of benign tumors were cystic lesions while in our study, 87.5% of the benign tumors were MFAMLs, and MFAMLs have the lowest ADCs among focal renal lesions;[23] and (ii) the benign lesions in Taouli's study included solid tumors, simple cysts, and renal abscesses etc., but the benign lesions in our study only included solid tumors.

Our results are consistent with other studies in the literature. For example, Cova et al.[5] reported that the mean ADC of solid renal tumors was significantly lower than that of normal renal parenchyma. Zhang et al.[25] showed that the value of ADC in normal renal parenchyma was higher than RCCs and angiomyolipomas by comparing the exponential ADCs and ADCs of 101 renal tumors to that of 20 healthy volunteers. Tanaka et al.[23] studied 41 solid renal tumors without visible macroscopic fat on unenhanced CT and DW-MRI, and observed that the mean and maximum ADC values of MFAMLs were significantly lower than those of ccRCCs ($P = 0.0030$ and 0.0009, respectively). A study by Rosenkrantz et al.[16] indicated that ADCs of high-grade ccRCC were significantly lower than that of low-grade ccRCC with a b value of 400 s/mm² and a b value of 800 s/mm² in 57 patients with pathologically proven ccRCC. Our study results also found the ADCs of high-grade ccRCCs were significantly lower than that of low-grade ccRCCs.

Our study had several advantages. First, by using consecutive patients in our prospective study, we reduced the selection bias. Second, our study focused on small solid renal tumors ≤4 cm in size, which correlates with T1a staging of renal malignant tumors. Early diagnosis of renal tumors leads to early intervention and subsequent improved prognosis in clinical practice.[26-28] Third, our study determined the most suitable b-value in DW-MRI to distinguish malignant from benign lesions using b values of 0, 50, 400, 600 s/mm² at 3.0T. We based our choice of b values on the theories that low b values ($b \leq 200$ s/mm²) would lead to intravoxel incoherent motion effects[29] contributing to the ADC values, high b values ($b \geq 800$ s/mm²) would lead a decreased signal-to-noise ratio, and multiple b values would improve the accuracy of ADCs. Jie et al.[30] showed that the use of high field strength resulted in greater sensitivity and specificity for the detection of prostate cancer with DWI.

There were some limitations in our study as well. First, since the sample size was relatively small and all RCCs included in our study were ccRCCs, our study did not compare the ADC of RCCs subtypes. Second, our study concentrated on solid renal tumors without evaluating the cystic renal lesions. Third, the cut-off ADC proposed in our study cannot be easily reproduced because it is dependent on the MR scanner and sequence, which are inherent limitations of DW-MRI. Thus, in the future, it will be necessary to establish standardized DW-MRI acquisition parameters and processing procedures.

In conclusion, our study has shown the potential of DW-MRI in differentiating ccRCCs from benign small solid renal tumors (≤4 cm), which when combined with nonenhanced MRI, could lead to an increase in accuracy for diagnosing ccRCCs.

References

1. Kessler O, Mukamel E, Hadar H, Gillon G, Konechezky M, Servadio C. Effect of improved diagnosis of renal cell carcinoma on the course of the disease. J Surg Oncol 1994;57:201-4.
2. Israel GM, Bosniak MA. Renal imaging for diagnosis and staging of renal cell carcinoma. Urol Clin North Am 2003;30:499-514.
3. Mehran R, Nikolsky E. Contrast-induced nephropathy: Definition, epidemiology, and patients at risk. Kidney Int Suppl 2006;(100):S11-5.
4. Sadowski EA, Bennett LK, Chan MR, Wentland AL, Garrett AL, Garrett RW, et al. Nephrogenic systemic fibrosis: Risk factors and incidence estimation. Radiology 2007;243:148-57.
5. Cova M, Squillaci E, Stacul F, Manenti G, Gava S, Simonetti G, et al. Diffusion-weighted MRI in the evaluation of renal lesions: Preliminary results. Br J Radiol 2004;77:851-7.
6. Squillaci E, Manenti G, Di Stefano F, Miano R, Strigari L, Simonetti G. Diffusion-weighted MR imaging in the evaluation of renal tumours. J Exp Clin Cancer Res 2004;23:39-45.
7. Zhang J, Tehrani YM, Wang L, Ishill NM, Schwartz LH, Hricak H. Renal masses: Characterization with diffusion-weighted MR imaging – a preliminary experience. Radiology 2008;247:458-64.
8. Doganay S, Kocakoç E, Ciçekçi M, Aglamis S, Akpolat N, Orhan I. Ability and utility of diffusion-weighted MRI with different b values in the evaluation of benign and malignant renal lesions. Clin Radiol 2011;66:420-5.
9. Sandrasegaran K, Sundaram CP, Ramaswamy R, Akisik FM, Rydberg MP, Lin C, et al. Usefulness of diffusion-weighted imaging in the evaluation of renal masses. AJR Am J Roentgenol 2010;194:438-45.
10. Moch H, Artibani W, Delahunt B, Ficarra V, Knuechel R, Montorsi F, et al. Reassessing the current UICC/AJCC TNM staging for renal cell carcinoma. Eur Urol 2009;56:636-43.
11. Edge SB, Compton CC. The American Joint Committee on Cancer: The 7th edition of the AJCC cancer staging manual and the future of TNM. Ann Surg Oncol 2010;17:1471-4.
12. Xian J, Du H, Wang X, Yan F, Zhang Z, Hao H, et al. Feasibility and value of quantitative dynamic contrast enhancement MR imaging in the evaluation of sinonasal tumors. Chin Med J 2014;127:2259-64.
13. Taouli B, Thakur RK, Mannelli L, Babb JS, Kim S, Hecht EM, et al. Renal lesions: Characterization with diffusion-weighted imaging versus contrast-enhanced MR imaging. Radiology 2009;251:398-407.
14. Wehrli NE, Kim MJ, Matza BW, Melamed J, Taneja SS, Rosenkrantz AB. Utility of MRI features in differentiation of central renal cell carcinoma and renal pelvic urothelial carcinoma. AJR Am J Roentgenol 2013;201:1260-7.
15. Kim S, Jain M, Harris AB, Lee VS, Babb JS, Sigmund EE, et al. T1 hyperintense renal lesions: Characterization with diffusion-weighted MR imaging versus contrast-enhanced MR imaging. Radiology 2009;251:796-807.
16. Rosenkrantz AB, Niver BE, Fitzgerald EF, Babb JS, Chandarana H, Melamed J. Utility of the apparent diffusion coefficient for distinguishing clear cell renal cell carcinoma of low and high nuclear grade. AJR Am J Roentgenol 2010;195:W344-51.
17. Notohamiprodjo M, Staehler M, Steiner N, Schwab F, Sourbron SP, Michaely HJ, et al. Combined diffusion-weighted, blood oxygen level-dependent, and dynamic contrast-enhanced MRI for characterization and differentiation of renal cell carcinoma. Acad Radiol 2013;20:685-93.
18. Kim JH, Bae JH, Lee KW, Kim ME, Park SJ, Park JY. Predicting the histology of small renal masses using preoperative dynamic contrast-enhanced magnetic resonance imaging. Urology 2012;80:872-6.
19. Mileto A, Marin D, Ramirez-Giraldo JC, Scribano E, Krauss B, Mazziotti S, et al. Accuracy of contrast-enhanced dual-energy MDCT for the assessment of iodine uptake in renal lesions. AJR Am J Roentgenol 2014;202:W466-74.
20. Kim EY, Park BK, Kim CK, Lee HM. Clinico-radio-pathologic features of a solitary solid renal mass at MDCT examination. Acta Radiol 2010;51:1143-8.
21. Boyd AS, Zic JA, Abraham JL. Gadolinium deposition in nephrogenic fibrosing dermopathy. J Am Acad Dermatol 2007;56:27-30.
22. Morcos SK, Thomsen HS, Webb JA. Contrast-media-induced nephrotoxicity: A consensus report. Contrast Media Safety Committee, European Society of Urogenital Radiology (ESUR). Eur Radiol 1999;9:1602-13.
23. Tanaka H, Yoshida S, Fujii Y, Ishii C, Tanaka H, Koga F, et al. Diffusion-weighted magnetic resonance imaging in the differentiation of angiomyolipoma with minimal fat from clear cell renal cell carcinoma. Int J Urol 2011;18:727-30.
24. Chan JH, Tsui EY, Luk SH, Fung SL, Cheung YK, Chan MS, et al. MR diffusion-weighted imaging of kidney: Differentiation between hydronephrosis and pyonephrosis. Clin Imaging 2001;25:110-3.
25. Zhang YL, Yu BL, Ren J, Qu K, Wang K, Qiang YQ, et al. EADC Values in Diagnosis of Renal Lesions by 3.0 T Diffusion-weighted Magnetic Resonance Imaging: Compared with the ADC Values. Appl Magn Reson 2013;44:349-63.
26. Agnello F, Roy C, Bazille G, Galia M, Midiri M, Charles T, et al. Small solid renal masses: Characterization by diffusion-weighted MRI at 3 T. Clin Radiol 2013;68:e301-8.
27. Patel HD, Kates M, Pierorazio PM, Hyams ES, Gorin MA, Ball MW, et al. Survival after diagnosis of localized T1a kidney cancer: Current population-based practice of surgery and nonsurgical management. Urology 2014;83:126-32.
28. Sun M, Becker A, Tian Z, Roghmann F, Abdollah F, Larouche A, et al. Management of localized kidney cancer: Calculating cancer-specific mortality and competing risks of death for surgery and nonsurgical management. Eur Urol 2014;65:235-41.
29. Jia QJ, Zhang SX, Chen WB, Liang L, Zhou ZG, Qiu QH, et al. Initial experience of correlating parameters of intravoxel incoherent motion and dynamic contrast-enhanced magnetic resonance imaging at 3.0 T in nasopharyngeal carcinoma. Eur Radiol 2014;24:3076-87.
30. Jie C, Rongbo L, Ping T. The value of diffusion-weighted imaging in the detection of prostate cancer: A meta-analysis. Eur Radiol 2014;24:1929-41.